Physics and Imaging in Radiation Oncology 18 (2021) 78–81

Contents lists available at ScienceDirect

Physics and Imaging in Radiation Oncology

journal homepage: www.sciencedirect.com/journal/physics-and-imaging-in-radiation-oncology

Short Communication

Delivery of online adaptive magnetic resonance guided radiotherapy based on isodose boundaries

Claudio Votta, Davide Cusumano, Luca Boldrini, Nicola Dinapoli *, Lorenzo Placidi, Gabriele Turco, Marco Valerio Antonelli, Veronica Pollutri, Angela Romano, Luca Indovina, Vincenzo Valentini

Dipartimento di Diagnostica per Immagini, Radioterapia Oncologica ed Ematologia, Fondazione Policlinico Universitario "A. Gemelli" IRCCS, 00168 Rome, Italy

ARTICLE INFO

Keywords:
Dosimetric boundary
MR-guided radiotherapy
Image guidance gating

ABSTRACT

Magnetic Resonance-guided Radiotherapy (MRgRT) allows direct monitoring of treated volumes. The aim of this study was to investigate the feasibility of a new gating strategy consisting in using an isodose as boundary. Forty-four patients treated for thoracic and abdominal lesions using MRgRT were enrolled. The accuracy of the new strategy was compared to the conventional one in terms of area improvement available for gating without compromising target coverage. A mean increase of 24% for lung, 15% for liver and 11% for pancreas was observed, demonstrating how the new method can be useful in challenging situations with low dose conformality.

1. Introduction

Recent technological developments in the field of radiation oncology led to the introduction of new hybrid systems, able to combine the delivery precision of a modern linear accelerator with the image quality of Magnetic Resonance (MR) imaging [1–3]. Besides enhanced positioning imaging quality, these systems allow to reduce inter-fraction treatment variability owing to a dedicated online adaptive workflow and to efficaciously manage intrafraction organ motion, required for real-time MR imaging and advanced gating strategies [4,5].

Several recent studies quantified tumor motion during treatment and demonstrated the occurrence of effects which may happen during a treatment fraction, such as modified target trajectories with movement of the tumor outside the high dose region [6,7]. For this reason, both passive and active strategies have been developed to safely manage tumor motion during therapy, reporting different levels of reliability and robustness [8–11]. With the introduction of Magnetic Resonance-guided Radiotherapy (MRgRT), direct monitoring of tumor motion during treatment delivery has become possible: hybrid MR-Linacs allow the continuous acquisition of planar MR images during treatment with up to 8 frames/second on a single sagittal plane or with 5 frames/second on three orthogonal plans [5,12].

As MR images are acquired in 2D-cine mode, in clinical practice often a tolerance region (boundary) is defined to stop the radiation beam as soon as the target structure moves beyond this region. This gating strategy can either be managed automatically or manually by a radiation therapist. A visual scheme of the gating functionality is reported in Supplementary materials. Automatic gating commonly uses Clinical Target Volume (CTV) as target structure and its isotropic geometric expansion, which frequently coincides with the Planning Target Volume (PTV), as boundary region [13–16].

The possibility of indirect CTV monitoring using nearby anatomical reference structures (i.e. organs at risk, OARs) has also been explored with interesting results in selected clinical scenarios [17,18]. Despite its wide diffusion, the strategy of using the CTV as target structure and its isotropic expansion as boundary can lead to suboptimal results, as the treated volume inside the prescribed isodose may not match with an isotropic structure. For example in pancreatic lesions, the anatomical proximity of several radiosensitive OARs to the tumor (e.g., duodenum, stomach and bowel loops) leads to highly irregular dose distributions cause of the anatomy and location of the target [19,20]. In these cases, the use of an isotropic boundary can be misleading allowing beam delivery also when the tumor is located outside the high dose region; this can result in decreased target coverage and increased risk of toxicity.

To the best of our knowledge no alternative approaches to prevent such effect during MRgRT delivery are available. The aim of this study

* Corresponding author.
E-mail address: nicola.dinapoli@policlinicogemelli.it (N. Dinapoli).

https://doi.org/10.1016/j.phro.2021.05.005
Received 15 June 2020; Received in revised form 14 May 2021; Accepted 19 May 2021
Available online 7 June 2021

was to investigate an alternative strategy to manage beam delivery in cases where the high dose region significantly differs from the geometric expansion of the CTV. Therefore, the use of an isodose line as alternative boundary was compared to conventional isotropic boundaries for different stereotactic body radiotherapy (SBRT) treatments of thoracic and abdominal lesions.

2. Material and methods

Forty-four patients treated for thoracic and abdominal lesions were retrospectively enrolled in this study (17 lung, 17 liver and 10 pancreatic lesions). All the patients underwent a MRgRT treatment delivered in 3 to 8 fractions on 0.3 T MRgRT system (MRIdian, ViewRay, Mountain View, California, USA) from June 2019 to February 2020 and signed a specific informed consent for therapy delivery and use of therapy imaging for our study.

All MRgRT treatments were administered in breath hold conditions by monitoring the tumor position during the entire therapy by means of 2D-MR images acquired in cine modality with 4 frames/second. No GTV to CTV margin was foreseen and PTV was defined by adding a 3 mm isotropic margin to the CTV. Dose calculation was performed with a Monte Carlo algorithm with a grid resolution of 0.2 cm and the beam energy was 6 MeV [21].

MR images were acquired on the sagittal plane passing through the geometrical center of the GTV using a true fast imaging (TRUFI) sequence, with 5 mm slice thickness, 35x35 cm^2 field of view, T2*/T1 image contrast and spatial resolution of 3.5x3.5 mm^2 [22,23].

Owing to automatic gating, the contours of the target structure were automatically deformed and projected onto the different cine frames as well as the boundary structure, which was rigidly transferred to the cine MR frames. The radiation beam was automatically turned off whenever a predefined percentage of the target structure (set equal to 5% in this study) moved out of the boundary. A visual scheme of the gating functionality is reported in Supplementary materials.

Treated volume was defined for each treatment plan as the volume enclosed by the Reference Isodose (RI) and represented the dose value taken into consideration to evaluate the target coverage of the treatment [24]. The RI was set equal to the 95% of the prescribed dose for the plans normalized at 50% of the target structure, while it was coincident with the prescribed dose for the plans normalized to an isodose volume, as suggested by ICRU 91[25]. Treatment plans were classified as function of their conformality, defined using the conformation number (CN) [26,27].

$$CN = \frac{TV_{RI}{}^2}{TV \times V_{RI}}$$

Here, the PTV represents the Target Volume (TV), V_{RI} represents the volume of reference isodose and TV_{RI} the TV covered by the reference isodose, corresponding to the intersection between PTV and V_{RI}.

Based on the CN value, treatment plans were classified in plans with low ($CN \leq 0.6$), moderate ($0.6 < CN \leq 0.7$) or high ($CN > 0.7$) conformality. Boundary analysis was performed comparing the area covered by the PTV in the gating plane with the area covered by the RI on the same plane.

The degree of overlap between PTV and RI on the gating plane was quantified in terms of Hausdorff distance (HD) and Dice index, calculated between the reference isodose and the PTV area using MIM software (version 7.0.4, MIM software Inc, United States) [28,29]. The difference between the two boundaries was considered significant for Dice values lower than 0.9. In the evaluation of the importance of using a dosimetric boundary at different plan complexity levels, the correlation between Dice, HD and CN was quantified using Spearman's correlation test [30]. All the statistical analyses were performed using R software (version 3.6.1, R Core Team, Austria).

3. Results

The observed dose distribution conformality was low in two of the selected plans, moderate in 44 and high in 18 cases. As regards the dose conformality, the lowest median CN values was observed in case of pancreatic (0.7) and lung lesions (0.7), while higher values were obtained of liver (0.7).

The median values and the corresponding ranges for the different parameters chosen to compare the PTV and reference isodose volume (RIV) boundary were reported in Table 1, separately for each anatomical site, while detailed values were reported as Supplementary material.

The area covered by RI was generally larger than the PTV area, with a mean increase of 24% for lung, 15% for liver and 11% for pancreatic lesions: only in three pancreatic cases an RI area smaller than PTV was observed, mainly due to the presence of radiosensitive OAR in close proximity to the target.

Concerning HD analysis, higher values were observed in pancreatic lesions (median value equal to 6.8 mm) with respect to liver (3.0 mm) and lung (2.8 mm), demonstrating a larger difference in using the two strategies in case of pancreas, as also supported by the lowest value in terms of percentage degree of overlapping (11% in pancreas, 15% in liver and 25% in lung).

Overall, on the basis of the geometric analysis performed, a significant difference in using the RI with respect the PTV as boundary was observed in 22 of the investigated cases, with a larger impact observed in case of pancreatic lesions (8/10) with respect lung (12/17) and liver (2/17).

Spearman's correlation analysis showed a high correlation ($R = 0.8$) between the Dice index and the CN of the treatment plan, independently from the treatment site investigated, while no significant correlation was observed between HD and CN ($R = -0.3$).

4. Discussion

In this study, the use of a treated isodose boundaries as gating structure for MRgRT was investigated in comparison to conventional standard strategy consisting in using an isotropic expansion of the target structure.

The analysis highlighted limited differences between the two strategies for treatment plans characterized by dose distributions of high conformality (only 4/18 plans with $CN \geq 0.7$ reported a Dice index < 0.9), while larger differences were observed in plans with low conformality (23/26 plans with a $CN < 0.7$ reported a Dice index < 0.9).

Gating efficiency is a relevant and contemporary topic in MRgRT, as time represents a key-factor to clinically manage as many patients as possible with these hybrid machines, as demonstrated in literature describing experiences in both low and high field units [31,32].The accuracy of treatment delivery, using a geometrical boundary, was firstly studied by van Sörnsen de Koste et al observing that this strategy ensured high gating efficiency in 15 patients affected by abdominal and thoracic tumors, with the GTV inside the selected boundary for 67% to 87% of the total treatment time [33].To the best of our knowledge, no alternative gating strategy to geometric one gating has been reported in literature.

Using treated volume as boundary may further improve gating efficiency by stopping the treatment delivery only when the GTV moves outside the region receiving the prescribed dose, regardless of its geometric position with respect to PTV.

Dice analysis demonstrated relevant differences between the two strategies in the lung and pancreas, while this was not observed in the liver. Fig. 1 summarizes some real-life clinical scenarios in which the use of this strategy provides significant improvements in gating efficiency: the use of this strategy increases the area where treatment delivery is allowed, ensuring equivalent target coverage and increasing gating efficiency in lung lesions (Fig. 1a). Similarly, the application of the dosimetric boundary can avoid that target results are outside the high dose

Table 1
Median values of the indicators chosen to compare RI and PTV for single anatomical site. Dose values corresponding to the RI, PTV and CN of the treatment plans were reported as SBRT plan indicators.

		Dosimetric Indicators			Geometric Indicators			
		RI Gy	PTV cc	CN	DICE	Δ Area (RIV-PTV) cm^2	%	HD mm
Lung	Median	47.5	2.8	0.7	0.8	0.6	24	2.8
	Range	39.9 / 50	1 / 38	0.5 / 0.8	0.7 / 0.8	0.0 / 1.9	1 / 48	1.5 / 12.1
Liver	Median	47.5	14.0	0.7	0.9	0.9	15	3.0
	Range	22.8 / 51.3	4.3 / 75.3	0.6 / 0.9	0.8 / 0.9	0.3 / 2.9	2 / 30	2.8 / 6.0
Pancreas	Median	40.0	37.6	0.7	0.8	1.2	11	6.8
	Range	30 / 44	7.3 / 74.7	0.5 / 0.8	0.8 / 0.9	−1.9 / 3.6	−2 / 35	3.1 / 11.9

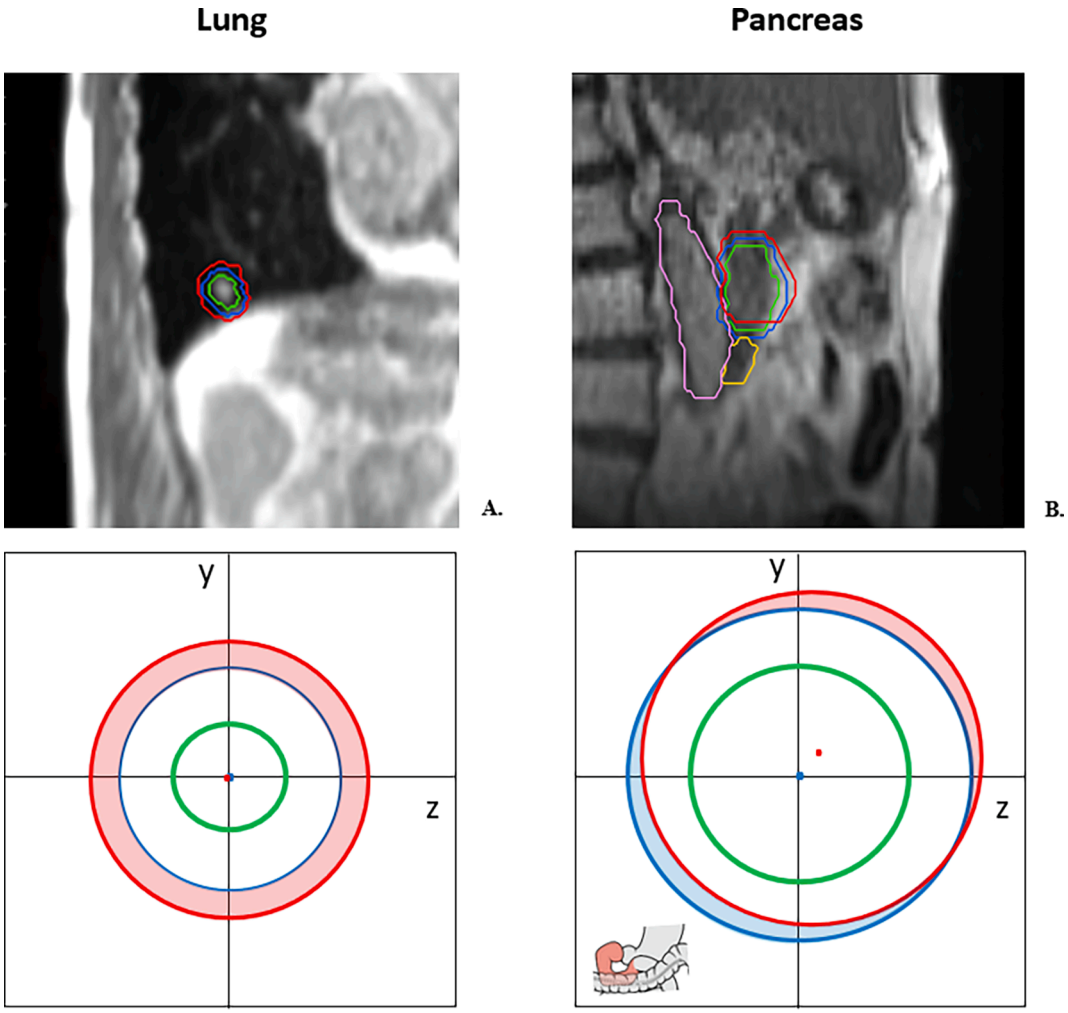

Fig. 1. Schematic impact using a reference isodose as boundary in the treatment of lung and pancreatic lesions. Top: sagittal plan views. Bottom: comparison of the area covered by reference isodose (red) and PTV (blue). (For interpretation of the references to colour in this figure legend, the reader is referred to the web version of this article.)

region, but the system does not stop the beam delivery, as in the described case of pancreatic lesions (Fig. 1b).

Despite the promising results, this exploratory study has different limitations, which should be considered prior to transferring this procedure to clinical practice. Firstly, MR gating implemented in low field hybrid units is performed in a single sagittal plane; all considerations reported do not account for the left–right direction, for which the use of larger CTV-PTV margins remains to date the only effective strategy for motion compensation, as evidenced in various low field MRgRT experiences [8,34,35].Secondly, this is a retrospective analysis using plans of patients treated with the geometric boundary strategy, which limits the clinical impact of these observations. Further prospective studies including larger cohorts of patients are recommended to quantify the gain in terms of gating efficiency and treatment time reduction, which could be achieved introducing the dosimetric boundary strategy in daily clinical practice.

In conclusion, the use of the dosimetric boundary could allow to identify a boundary region with the advantage of directly reflecting the actual dose distribution, ensuring a gating region which could allow reduced treatment time in case of lung and liver lesions and to optimize the beam delivery in case of pancreatic ones.

Declaration of Competing Interest

The authors declare the following financial interests/personal relationships which may be considered as potential competing interests: Nicola Dinapoli: has received speaker honoraria by ViewRay company. Luca Boldrini: has received speaker honoraria by ViewRay company. Davide Cusumano: has received speaker honoraria by ViewRay company. Vincenzo Valentini: has received speaker honoraria by ViewRay company.

Acknowledgements

We would like to thank Franziska M. Lohmeyer, PhD, Fondazione Policlinico Universitario A. Gemelli IRCCS, for her support revising our manuscript.

This paper is part of a special issue that contains contributions originally submitted to the scientific meeting MR in RT, which was planned to take place 05/2020, organized by the German Research Center (DKFZ) in Heidelberg.

Appendix A. Supplementary data

Supplementary data to this article can be found online at https://doi.org/10.1016/j.phro.2021.05.005.

References

[1] Mutic S, Dempsey JF. The ViewRay system: magnetic resonance-guided and controlled radiotherapy. Semin Radiat Oncol 2014;24(3):196–9. https://doi.org/10.1016/j.semradonc.2014.02.008.
[2] Lagendijk JJW, Raaymakers BW, van Vulpen M. The magnetic resonance imaging-linac system. Semin Radiat Oncol 2014;24(3):207–9. https://doi.org/10.1016/j.semradonc.2014.02.009.
[3] Thorwarth D, Muren L. Imaging science and development in modern high-precision radiotherapy. Phys Imaging Radiat Oncol 2019;12:63–6. https://doi.org/10.1016/j.phro.2019.11.008.
[4] Boldrini L, Cusumano D, Cellini F, Azario L, Mattiucci GC, Valentini V. Online adaptive magnetic resonance guided radiotherapy for pancreatic cancer: state of the art, pearls and pitfalls. Radiat Oncol 2019;14:71. https://doi.org/10.1186/s13014-019-1275-3.
[5] van der Heide UA. MR-guided radiation therapy. Phys Med 2016;32:175. https://doi.org/10.1016/j.ejmp.2016.07.284.
[6] Dhont J, Harden SV, Chee LYS, Aitken K, Hanna GG, Bertholet J. Image-guided radiotherapy to manage respiratory motion: lung and liver. Clin Oncol 2020;32(12):792–804. https://doi.org/10.1016/j.clon.2020.09.008.
[7] Mirzapour SA, Mazur TR, Harold Li H, Salari E, Sharp GC. Technical Note: Cumulative dose modeling for organ motion management in MRI-guided radiation therapy. Med Phys 2021;48(2):597–604. https://doi.org/10.1002/mp.v48.210.1002/mp.14500.
[8] Cusumano D, Dhont J, Boldrini L, Chiloiro G, Romano A, Votta C, et al. Reliability of ITV approach to varying treatment fraction time: a retrospective analysis based on 2D cine MR images. Radiat Oncol 2020;15(1). https://doi.org/10.1186/s13014-020-01530-6.
[9] Wu VWC, Ng APL, Cheung EKW. Intrafractional motion management in external beam radiotherapy. J Xray Sci Technol 2020;27(6):1071–86. https://doi.org/10.3233/XST-180472.
[10] Korreman SS. Image-guided radiotherapy and motion management in lung cancer. Br J Radiol 2015;88(1051):20150100. https://doi.org/10.1259/bjr.20150100.
[11] Ge J, Santanam L, Noel C, Parikh PJ. Planning 4-dimensional computed tomography (4DCT) cannot adequately represent daily intrafractional motion of abdominal tumors. Int J Radiat Oncol Biol Phys 2013;85(4):999–1005. https://doi.org/10.1016/j.ijrobp.2012.09.014.
[12] Green OL, Rankine LJ, Cai B, Curcuru A, Kashani R, Rodriguez V, et al. First clinical implementation of real-time, real anatomy tracking and radiation beam control. Med Phys 2018;45(8):3728–40. https://doi.org/10.1002/mp.2018.45.issue-810.1002/mp.13002.
[13] Sahin B, Zoto Mustafayev T, Gungor G, Aydin G, Yapici B, Atalar B, et al. First 500 fractions delivered with a magnetic resonance-guided radiotherapy system: initial experience. Cureus 2019;11:e6457. https://doi.org/10.7759/cureus.6457.
[14] Klüter S, Katayama S, Spindeldreier CK, Koerber SA, Major G, Alber M, et al. First prospective clinical evaluation of feasibility and patient acceptance of magnetic resonance-guided radiotherapy in Germany. Strahlenther Onkol 2020;196(8):691–8. https://doi.org/10.1007/s00066-020-01578-z.
[15] Finazzi T, van Sörnsen de Koste JR, Palacios MA, Spoelstra FOB, Slotman BJ, Haasbeek CJA, et al. Delivery of magnetic resonance-guided single-fraction stereotactic lung radiotherapy. Phys Imaging Radiat Oncol 2020;14:17–23. https://doi.org/10.1016/j.phro.2020.05.002.
[16] Tetar SU, Bruynzeel AME, Lagerwaard FJ, Slotman BJ, Bohoudi O, Palacios MA. Clinical implementation of magnetic resonance imaging guided adaptive radiotherapy for localized prostate cancer. Phys Imaging Radiat Oncol 2019;9:69–76. https://doi.org/10.1016/j.phro.2019.02.002.
[17] Massaccesi M, Cusumano D, Boldrini L, Dinapoli N, Fionda B, Teodoli S, et al. A new frontier of image guidance: Organs at risk avoidance with MRI-guided respiratory-gated intensity modulated radiotherapy: technical note and report of a case. J Appl Clin Med Phys 2019;20:194–8. https://doi.org/10.1002/acm2.12575.
[18] Boldrini L, Cellini F, Manfrida S, Chiloiro G, Teodoli S, Cusumano D, et al. Use of Indirect Target Gating in Magnetic Resonance-guided Liver Stereotactic Body Radiotherapy: Case Report of an Oligometastatic Patient. Cureus 2018;10:e2292. doi: 10.7759/cureus.2292.
[19] Placidi L, Romano A, Chiloiro G, Cusumano D, Boldrini L, Cellini F, et al. On-line adaptive MR guided radiotherapy for locally advanced pancreatic cancer: Clinical and dosimetric considerations. Tech Innov Patient Support Radiat Oncol 2020;15:15–21. https://doi.org/10.1016/j.tipsro.2020.06.001.
[20] Bohoudi O, Bruynzeel AME, Senan S, Cuijpers JP, Slotman BJ, Lagerwaard FJ, et al. Fast and robust online adaptive planning in stereotactic MR-guided adaptive radiation therapy (SMART) for pancreatic cancer. Radiother Oncol 2017;125(3):439–44. https://doi.org/10.1016/j.radonc.2017.07.028.
[21] Wang Y, Mazur TR, Green O, Hu Y, Li H, Rodriguez V, et al. A GPU-accelerated Monte Carlo dose calculation platform and its application toward validating an MRI-guided radiation therapy beam model. Med Phys 2016;43(7):4040–52. https://doi.org/10.1118/1.4953198.
[22] Cusumano D, Boldrini L, Yadav P, Yu G, Musurunu B, Chiloiro G, et al. External validation of an early regression index (ERITCP) as predictor of pathological complete response in rectal cancer using MR-guided Radiotherapy. Int J Radiat Oncol Biol Phys 2020;108(5):1347–56. https://doi.org/10.1016/j.ijrobp.2020.07.2323.
[23] Hu Y, Rankine L, Green OL, Kashani R, Li HH, Li H, et al. Characterization of the onboard imaging unit for the first clinical magnetic resonance image guided radiation therapy system. Med Phys 2015;42(10):5828–37. https://doi.org/10.1118/1.4930249.
[24] Berthelsen AK, Dobbs J, Kjellén E, Landberg T, Möller TR, Nilsson P, et al. What's new in target volume definition for radiologists in ICRU Report 71? How can the ICRU volume definitions be integrated in clinical practice? Cancer Imaging 2007;7:104–16. https://doi.org/10.1102/1470-7330.2007.0013.
[25] International Commission on Radiation Units and Measurements (ICRU) n.d. https://icru.org/content/reports/icru-report-91-prescribing-recording-and-reporting-of-stereotactic-treatments-with-small-photon-beams (accessed May 30, 2020).
[26] Riet AV, Mak ACA, Moerland MA, Elders LH, van der Zee W. A conformation number to quantify the degree of conformality in brachytherapy and external beam irradiation: application to the prostate. Int J Radiat Oncol Biol Phys 1997;37(3):731–6. https://doi.org/10.1016/S0360-3016(96)00601-3.
[27] Paddick I. A simple scoring ratio to index the conformity of radiosurgical treatment plans. Technical note. J Neurosurg 2000;93(Suppl 3):219–22. https://doi.org/10.3171/jns.2000.93.supplement.
[28] Dice LR. Measures of the amount of ecologic association between species. Ecology 1945;26:297–302. https://doi.org/10.2307/1932409.
[29] Park JM, Park S-Y, Ye S-J, Kim JH, Carlson J, Wu H-G. New conformity indices based on the calculation of distances between the target volume and the volume of reference isodose. Br J Radiol 2014;87(1043):20140342. https://doi.org/10.1259/bjr.20140342.
[30] Taylor J. An Introduction to Error Analysis: The Study of Uncertainties in Physical Measurements. II. Sausalito, CA: University Science Books; 1997.
[31] Winkel D, Bol GH, Kroon PS, van Asselen B, Hackett SS, Werensteijn-Honingh AM, et al. Adaptive radiotherapy: the Elekta Unity MR-linac concept. Clin Transl Radiat Oncol 2019;18:54–9. https://doi.org/10.1016/j.ctro.2019.04.001.
[32] Placidi L, Cusumano D, Boldrini L, Votta C, Pollutri V, Antonelli MV, et al. Quantitative analysis of MRI-guided radiotherapy treatment process time for tumor real-time gating efficiency. J Appl Clin Med Phys 2020;21(11):70–9. https://doi.org/10.1002/acm2.v21.1110.1002/acm2.13030.
[33] van Sörnsen de Koste JR, Palacios MA, Bruynzeel AME, Slotman BJ, Senan S, Lagerwaard FJ. MR-guided gated stereotactic radiation therapy delivery for lung, adrenal, and pancreatic tumors: a geometric analysis. Int J Radiat Oncol Biol Phys 2018;102(4):858–66. https://doi.org/10.1016/j.ijrobp.2018.05.048.
[34] Cusumano D, Dhont J, Boldrini L, Chiloiro G, Teodoli S, Massaccesi M, et al. Predicting tumour motion during the whole radiotherapy treatment: a systematic approach for thoracic and abdominal lesions based on real time MR. Radiother Oncol 2018;129(3):456–62. https://doi.org/10.1016/j.radonc.2018.07.025.
[35] Klüter S. Technical design and concept of a 0.35 T MR-Linac. Clin Transl. Radiat Oncol 2019;18:98–101. https://doi.org/10.1016/j.ctro.2019.04.007.